

ARTICLE

Intravitreal delivery of AAV-NDI1 provides functional benefit in a murine model of Leber hereditary optic neuropathy

Naomi Chadderton^{*1}, Arpad Palfi^{1,4}, Sophia Millington-Ward^{1,4}, Oliverio Gobbo², Nora Overlack³, Matthew Carrigan¹, Mary O'Reilly¹, Matthew Campbell¹, Carsten Ehrhardt², Uwe Wolfrum³, Peter Humphries¹, Paul F Kenna¹ and G Jane Farrar¹

Leber hereditary optic neuropathy (LHON) is a mitochondrially inherited form of visual dysfunction caused by mutations in several genes encoding subunits of the mitochondrial respiratory NADH-ubiquinone oxidoreductase complex (complex I). Development of gene therapies for LHON has been impeded by genetic heterogeneity and the need to deliver therapies to the mitochondria of retinal ganglion cells (RGCs), the cells primarily affected in LHON. The therapy under development entails intraocular injection of a nuclear yeast gene NADH-quinone oxidoreductase (*NDI1*) that encodes a single subunit complex I equivalent and as such is mutation independent. *NDI1* is imported into mitochondria due to an endogenous mitochondrial localisation signal. Intravitreal injection represents a clinically relevant route of delivery to RGCs not previously used for *NDI1*. In this study, recombinant adenoassociated virus (AAV) serotype 2 expressing *NDI1* (AAV-*NDI1*) was shown to protect RGCs in a rotenone-induced murine model of LHON. AAV-*NDI1* significantly reduced RGC death by 1.5-fold and optic nerve atrophy by 1.4-fold. This led to a significant preservation of retinal function as assessed by manganese enhanced magnetic resonance imaging and optokinetic responses. Intraocular injection of AAV-*NDI1* overcomes many barriers previously associated with developing therapies for LHON and holds great therapeutic promise for a mitochondrial disorder for which there are no effective therapies.

European Journal of Human Genetics (2013) 21, 62–68; doi:10.1038/ejhg.2012.112; published online 6 June 2012

Keywords: AAV; LHON; *NDI1*; gene therapy; mitochondria; retina

INTRODUCTION

Leber hereditary optic neuropathy (LHON) is a maternally inherited disorder affecting 1/25 000 people, predominantly males.¹ Loss of central vision results from degeneration of the retinal ganglion cell (RGC) layer and optic nerve.² In over 95% of patients the genetic pathogenesis of LHON involves mutations in genes encoding components of the mitochondrial respiratory NADH-ubiquinone oxidoreductase complex³ (complex I), involved in transfer of electrons from NADH to ubiquinone (coenzyme Q). Complex I is composed of 46 subunits, 7 of which are encoded by the mitochondrial genome, *ND1-6* and *ND4L*. Mutations in five mitochondrially encoded subunits, *ND1*, *ND4*, *ND4L*, *ND5* and *ND6*, are associated with LHON (<http://www.mitomap.org/MITOMAP>). There is growing evidence that mitochondrial dysfunction may be involved in a range of neurodegenerative disorders such as Alzheimer disease (AD), Huntington disease and dominant optic atrophy.⁴ It is not surprising that the retina with the most significant energy requirements of any mammalian tissue⁵ may be particularly vulnerable to mitochondrial dysfunction. However, such a dependency on energy may provide an opportunity for development of therapeutic interventions where a shift in energy metabolism may give rise to beneficial effects.

Complex I dysfunction results in an increase of reactive oxygen species and a decreased energy supply.⁶ ATP synthesis is coupled to oxygen consumption by the proton electrochemical gradient established across the mitochondrial inner membrane during oxidative phosphorylation⁷ (OXPHOS). Mitochondrial complex I mutations leading to respiratory chain dysfunction are linked to reduced oxygen consumption, a measure of overall mitochondrial activity.

Development of gene therapies for LHON has been impeded by a need to deliver therapies to mitochondria and the presence of intragenic heterogeneity. In this study, these impediments have been overcome using a nuclear gene NADH-quinone oxidoreductase (*NDI1*) from yeast (*Saccharomyces cerevisiae*) encoding a single subunit complex I equivalent, which is imported into mitochondria.⁸ A nuclear complementation approach using *NDI1* has been considered as a potential therapy for Parkinson's disease (PD).⁹ In addition, recombinant adenoassociated virus (AAV) serotype 5 delivery of *NDI1* into the optic layer of the superior colliculus of the brain has recently been shown to provide benefit in a chemically induced rat model of LHON.¹⁰ Although this represents an innovative strategy making use of transkingdom gene therapy, the mode of delivery is unlikely to be translatable to human LHON patients.

¹School of Genetics and Microbiology, Smurfit Institute of Genetics, Trinity College Dublin, Dublin, Ireland; ²School of Pharmacy and Pharmaceutical Sciences, Trinity College Dublin, Dublin, Ireland; ³Department of Cell and Matrix Biology, Institute of Zoology, Johannes Gutenberg University of Mainz, D-55099 Mainz, Germany

*Correspondence: Dr N Chadderton, School of Genetics and Microbiology, Smurfit Institute of Genetics, Trinity College Dublin, Dublin 2, Ireland. Tel: +353 1 8962482; Fax: +353 1 8963848; E-mail: chaddern@tcd.ie

⁴These authors contributed equally to this work.

Received 27 December 2011; revised 20 April 2012; accepted 26 April 2012; published online 6 June 2012

Given a scarcity of transgenic models for mitochondrial disorders¹¹ chemically induced models, based on the specific and irreversible complex I inhibitor rotenone, have been used in studies of PD, AD and LHON.^{12–16} Rotenone inhibits the reduction of ubiquinone and when administered intravitreally to mice, causes biochemical, structural and functional retinal deficits resembling those observed in LHON patients, notably loss of RGCs and degeneration of the optic nerve.^{15–17}

In this study, intraocular delivery of *NDI1* has been used to protect RGCs in a rotenone-induced murine model of LHON. Recombinant AAV serotype 2 (AAV2/2) expressing *NDI1* from a CMV promoter (AAV-*NDI1*) was administered to mice using a single intravitreal injection. AAV2/2 administered through this route has been shown to infect RGCs efficiently,^{18–20} resulting in a broad area of retinal transduction as the vitreous contacts the entire underlying retinal surface.²¹ Intravitreal injection of AAV provides a route of administration for the gene therapy, which is directly applicable to human patients and is routinely used to administer drugs such as Avastin and Lucentis for wet AMD. In summary, intravitreal injection of AAV-*NDI1* significantly reduced RGC death and optic nerve atrophy seen in untreated eyes and led to a preservation of retinal function as assessed by manganese (Mn^{2+}) enhanced magnetic resonance imaging (MEMRI) and optokinetic responses (OKR).

MATERIALS AND METHODS

AAV production

Yeast *NDI1* (accession no.: NM_001182483.1) was cloned as described²² downstream of the CMV immediate early promoter (pcDNA3.1-, Invitrogen, Paisley, UK) with a minimal poly-adenylation signal²³ to create pAAV-*NDI1*; Supplementary Figure 1. pAAV-*EGFP* was cloned as described.²⁴ Recombinant AAV2/2 viruses, AAV-*NDI1* and AAV-*EGFP* were generated by the Gene Vector production Centre of Nantes. Genomic titres were determined as described.²⁴

Mitochondrial isolation, western blot and respiratory analysis

Mitochondria were isolated from HeLa cells using Anti-TOM22 microbeads (Mitochondria isolation kit, Miltenyi Biotec GmbH, Bergisch Gladbach, Germany) and western blot and respiratory analysis performed as described in Supplementary Text.

Animals, intravitreal injections and histology

Wild-type 129 S2/SvHsd (Harlan UK Ltd, Oxfordshire, UK) mice were maintained under specific pathogen-free housing conditions. Intravitreal injections were carried out in strict compliance with the European Communities Regulations 2002 and 2005 (Cruelty to Animals Act) and the Association for Research in Vision and Ophthalmology statement for the use of animals. Adult mice were anaesthetised and pupils dilated as described.²⁵ Using topical anaesthesia (Amethocaine), a small puncture was made in the sclera. A 34-gauge blunt-ended microneedle attached to a 10- μ l Hamilton syringe was inserted through the puncture, and 0.6 μ l 2.5 mM rotenone (1.5 nmol) in dimethyl sulfoxide (DMSO, vehicle), 0.6 μ l DMSO alone or 3 μ l 1×10^{12} vp/ml AAV2/2 was slowly, over a 2-min period, administered into the vitreous. Following intravitreal injection, an anaesthetic reversing agent (100 mg/10 g body weight; atipamezole hydrochloride) was delivered by intraperitoneal injection. Body temperature was maintained using a homeothermic heating device. Animals were killed as described in the results. Eyes were processed for RNA extraction or light and electron microscopy analysis, and optic nerves were processed for light and electron microscopy as described^{24,26,27} (Supplementary Text).

Magnetic resonance imaging

Optic nerve integrity in experimental and control mice was assessed by MEMRI^{28–31} using a 7-T Bruker Biospec 70/30 magnet (Bruker Biospin, Ettlingen, Germany). MEMRI demarcates active regions of the brain due to the

ability of Mn^{2+} ions to enter excitable cells through voltage-gated calcium channels,²⁸ thus analysis of Mn^{2+} transport through the optic nerve provides a good measure of its integrity. Two hours before scanning, mice were anaesthetised and intravitreally injected, as described, with 2 μ l of 20 mg/ml manganese chloride ($MnCl_2$) in phosphate buffered saline (PBS). The $MnCl_2$ dose used was comparable to previous studies.^{30,31} Log signal intensities from MRI scans corresponding to the region immediately superior to the optic chiasm were quantified using the Image J software³² (<http://imagej.nih.gov/ij/>) (Supplementary Text).

Optokinetics

OKR spatial frequency thresholds were measured blind by two independent researchers using a virtual optokinetic system (VOS, OptoMotry, Cerebral Mechanics, Lethbridge, Alberta, Canada) as described³³ (Supplementary Text).

Statistical analysis

Data sets of treated and untreated samples were pooled, averaged and SD values calculated. Statistical significance of differences between data sets was determined by either Student's two-tailed *t*-test or analysis of variance (ANOVA) used with Tukey's multiple comparison *post hoc* test. In addition, the Kruskal–Wallis one-way ANOVA was applied to the MRI data set and Mann–Whitney *U*-tests were undertaken on all other data sets to establish that statistical significance was maintained using nonparametric statistical models. Analysis was performed using the Prism v. 5.0c (GraphPad Software, La Jolla, CA, USA); differences of $P < 0.05$ were considered statistically significant.

RESULTS

The focus of this study was to determine whether *NDI1* could rescue the complex I deficiency in a mouse model of LHON using a clinically relevant mode of delivery, intravitreal injection and an AAV serotype previously used in human clinical trials for another retinal disorder (Leber congenital amaurosis (LCA)). Central to the approach was the hypothesis that AAV2/2-mediated intravitreal delivery of the nuclear-encoded gene *NDI1* would result in therapeutically relevant levels of Ndi1 protein within RGC mitochondria. Owing to the low number of RGCs present in murine retina (~60 000 RGCs in 129/J mice³⁴) mitochondrial localisation of Ndi1 expressed from pAAV-*NDI1* was initially confirmed in HeLa cells by western blot analysis (56 kDa;³⁵ Supplementary Figure 2A). In addition, the ability of the *NDI1* transgene to protect cells from the effects of complex I inhibition following rotenone administration was assessed by analysis of oxygen consumption rates in transfected HeLa cells with and without rotenone treatment (Supplementary Figures 2B and C). As OXPHOS is the primary cause of oxygen consumption in mammalian cells, quantification of overall oxygen consumption provides an indirect measurement of mitochondrial activity. Respiratory measurements of control cells with and without rotenone were 16.85 ± 5.73 pmol/(s \times ml) and 62.17 ± 10.73 pmol/(s \times ml), respectively, giving a rotenone insensitive respiration percentage of $27.14 \pm 7.84\%$. In comparison, the percentage of rotenone insensitive respiration from AAV-*NDI1*-transfected cells was over 2.5-fold greater, $72.37 \pm 9.85\%$ ($P < 0.001$, $n = 6$; 61.81 ± 10.94 pmol/(s \times ml) and 85.54 ± 11.36 pmol/(s \times ml) with and without rotenone, respectively). These data suggest that AAV-*NDI1* provides significant protection from rotenone inhibition. Subsequent to evaluation of AAV-*NDI1* *in vitro*, 3×10^9 vp AAV-*NDI1* or 3×10^9 vp AAV-*EGFP* were intravitreally injected into adult mice and 2 weeks post-injection retinas were harvested and RNA extracted ($n = 6$). *In vivo* expression of *NDI1* mRNA was confirmed by RT-PCR (Supplementary Figure 2D).

Intravitreal injection of AAV2/2 mediates efficient transgene delivery to RGCs,^{18–20} with optimal expression obtained 3 weeks post-injection.^{18,19} Initially, this was verified using AAV2/2-*EGFP*.

Adult wild-type mice were intravitreally injected with 3×10^9 vp AAV-EGFP ($n=3$). Three weeks post-injection, retinas were analysed for the presence of EGFP and widespread expression of EGFP in the ganglion cells was detected (Figure 1). In addition to the cell bodies, a large number of EGFP-positive processes in the inner plexiform layer were also detected (Figures 1c and f). Ganglion cell axons were also positive for EGFP, these axons were readily detected both on the inner surface of the retina and in the optic nerve (Figures 1b and e). Furthermore, interneurons in the inner nuclear layer were also transduced by AAV2/2-EGFP (Figures 1b, c, e and f). The breadth and intensity of EGFP expression detected resulted in 3×10^9 vp AAV being used in the subsequent studies.

To establish if AAV-mediated *NDI1* levels in RGCs were sufficient to protect against rotenone insult, adult wild-type mice were intravitreally injected into contralateral eyes with 3×10^9 vp AAV-*NDI1* (and 3×10^8 vp AAV-EGFP, to facilitate identification of transduced regions of the retina) or with 3×10^9 vp AAV-EGFP alone ($n=4$). Three weeks post-injection, 1.5 nmol of rotenone was administered intravitreally to both eyes. Rotenone was added at this timepoint to ensure maximal expression of *Ndi1* in RGCs.^{18,19} Three weeks post-rotenone treatment retinal morphology was analysed (Figure 2). Sections from control eyes that had received AAV-EGFP (Figures 2b and d) demonstrated significant RGC degeneration that was not apparent in AAV-*NDI1*-treated retinas (Figures 2a and c). Notably, RGC counts were significantly greater in AAV-*NDI1*-treated retinas ($88.76 \pm 15.18 \text{ mm}^{-2}$) than in AAV-EGFP-treated retinas ($57.18 \pm 12.79 \text{ mm}^{-2}$; $P < 0.001$, $n=4$; Figure 2e). As complex I-linked LHON manifests as both a degeneration of the RGCs and optic nerve,¹⁷ it was important to examine whether the protection afforded to RGCs by AAV-*NDI1* was also exhibited in the optic nerve.

Optic nerves from mice, which had received AAV-*NDI1* in one eye and AAV-EGFP in the other and subsequently rotenone in both eyes (as above), were compared using transmission electron microscopy 3 weeks post-rotenone injection. At low-magnification uncharacteristic electron-dense structures not seen in non-rotenone-treated optic nerves (Supplementary Figure 3) were observed in rotenone-treated optic nerves (arrow heads, Figures 3a and b). These were less abundant in AAV-*NDI1*-treated optic nerves (Figure 3a) compared with AAV-EGFP-treated optic nerves (Figure 3b). At higher magnification the electron-dense structures were revealed to be disorganised membrane debris (Figure 3c), indicating that AAV-*NDI1* treatment had provided protection from degeneration to the optic nerves. Numbers of electron-dense structures were significantly less abundant in AAV-*NDI1*-treated mice (264.0 ± 72.9) compared with control, AAV-EGFP-treated mice (588.7 ± 29.8 ; $P < 0.01$, $n=3$; Figure 3d). To analyse long-term changes to the optic nerve post-treatment, optic nerves were collected 9 months post-rotenone injection from AAV-*NDI1*- and AAV-EGFP-treated mice. The thickness of the optic nerves was assessed in sections by light microscopy. The mean diameter of the optic nerves was significantly greater in AAV-*NDI1*-treated mice than in mice treated with AAV-EGFP (336.6 ± 14.5 and $247.7 \pm 56.7 \mu\text{m}$, respectively; $P < 0.01$, $n=3$; Figure 3e). These data demonstrate that intravitreal administration of AAV-*NDI1* provided significant morphological protection to both the retina and optic nerve from rotenone-induced complex I inhibition.

To determine whether the morphological protection afforded by AAV-*NDI1* translated into greater functional integrity in the LHON model, MEMRI was undertaken. MEMRI demarcates active regions of the brain due to the ability of Mn^{2+} to enter excitable cells through

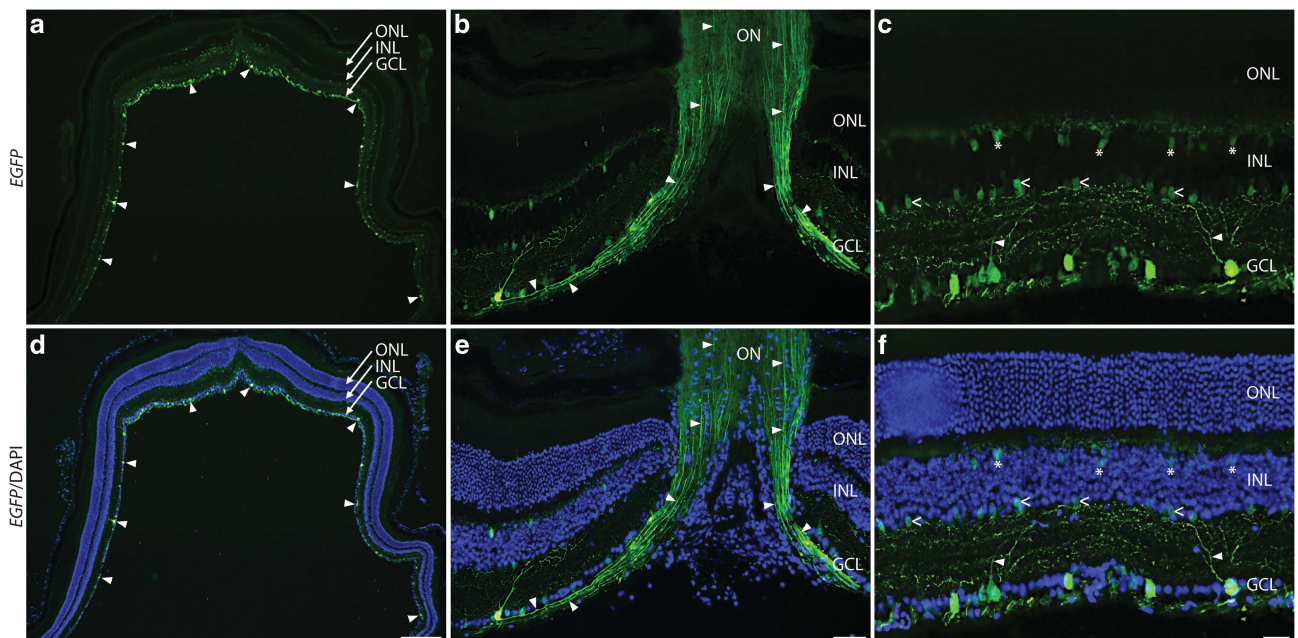


Figure 1 Histology of EGFP-treated retinas. Adult wild-type mice were intravitreally injected with 3×10^9 vp AAV-EGFP ($n=3$). Three weeks post-injection, eyes were enucleated, fixed, cryosectioned ($12 \mu\text{m}$) and nuclei counterstained with DAPI (blue); (a–c): EGFP signal; (d–f) EGFP and DAPI signals overlaid. (a, d) Overview of the retina indicating transduction coverage; arrowheads indicate transduced cells in the ganglion cell layer (GCL). (b, e) High-magnification view of the optic nerve head; arrowheads indicate EGFP-positive axons converging from the inner retinal surface to the optic nerve. (c, f) Detailed view of the retina indicating the transduced (EGFP-positive) cell populations. Arrowheads indicate the apical dendrite of the ganglion cells; open arrowheads indicate interneurons in the inner border of the inner nuclear layer (INL); Asterisks (*) indicate interneurons in the outer border of the INL. Many neuronal processes are also positive for EGFP in both the inner plexiform layers (IPL) and the outer plexiform layer (OPL). ONL, outer nuclear layer. Scale bars (d–f): 250, 50 and $25 \mu\text{m}$, respectively.

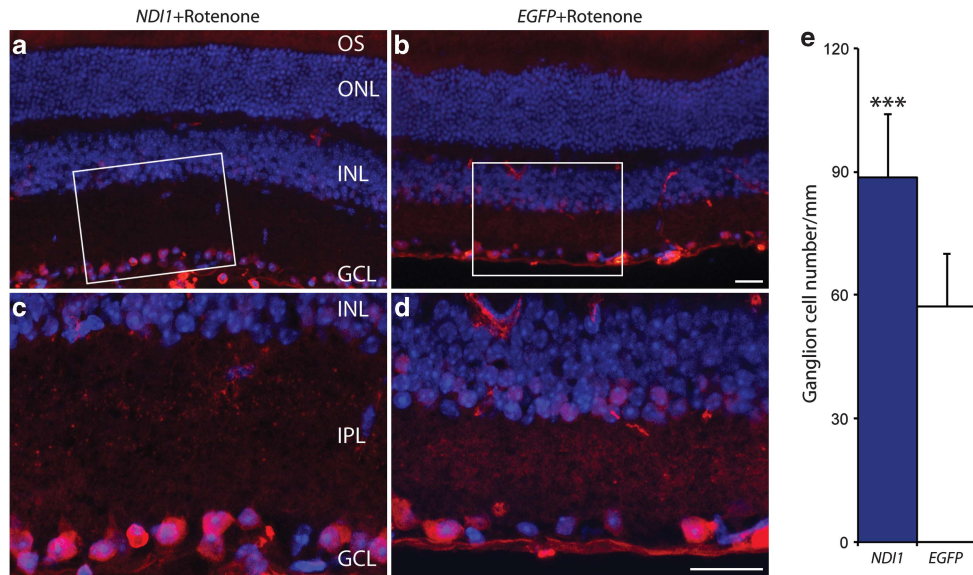


Figure 2 Histology of *ND11*-treated retinas following rotenone insult. Adult wild-type mice were intravitreally injected into contralateral eyes with 3×10^9 vp AAV-*ND11* (a, c) and 1×10^8 vp AAV-*EGFP* (EGFP signals not shown), to facilitate localisation of transduced regions of the retinas, or 3×10^9 vp AAV-*EGFP* (b, d) alone ($n=4$). Three weeks post-injection, 1.5 nmol of rotenone was administered intravitreally to both eyes. Three weeks post-rotenone treatment eyes were enucleated, fixed, cryosectioned ($12 \mu\text{m}$) and processed for immunocytochemistry using NeuN primary and Cy3-conjugated secondary antibodies (red). Nuclei were counterstained with DAPI (blue). (a, b) Overview of retinal histology with or without *ND11* treatment, respectively (light microscopy). (c, d) Detailed view of the ganglion cell (GCL) and inner plexiform (IPL) layers (laser confocal microscopy). Rectangles in a and b demark the areas shown in greater detail in c and d, respectively. ONL, outer nuclear layer; OS, photoreceptor outer segments. Scale bar: $20 \mu\text{m}$. (e) Bar chart representing mean ganglion cell counts per $100 \mu\text{m}$. Blue and white columns represent values corresponding to AAV-*ND11* + rotenone (*ND11*) and AAV-*EGFP* + rotenone (*EGFP*), respectively. Error bars represent SD values and $***P < 0.001$.

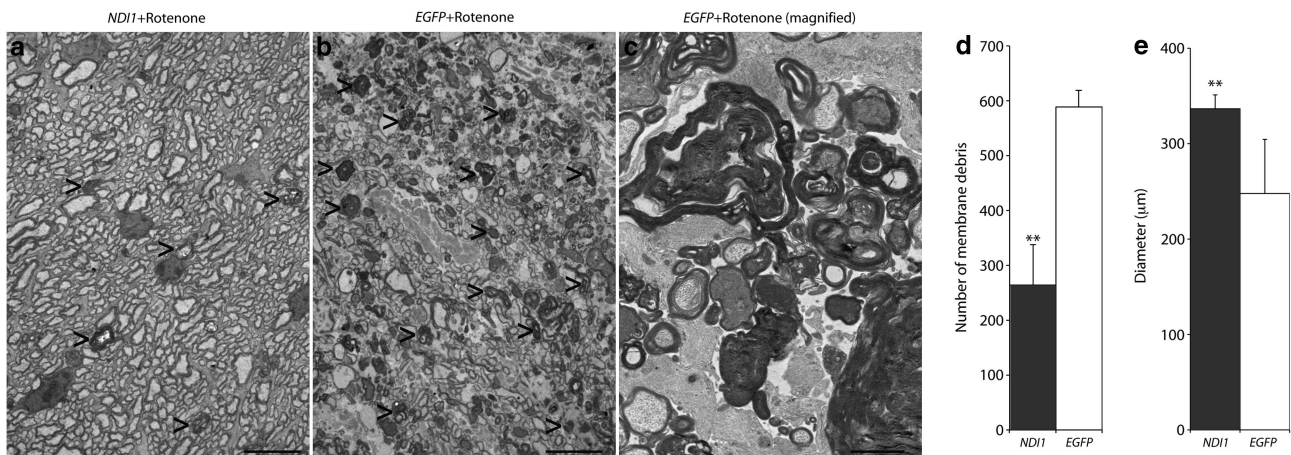


Figure 3 Ultra-structural analysis of *ND11*-treated optic nerves following rotenone insult. Adult wild-type mice were intravitreally injected into contralateral eyes with AAV-*ND11* (a) or AAV-*EGFP* (b, c) ($n=3$). Three weeks post-injection, 1.5 nmol of rotenone was administered intravitreally to both eyes. After 3 weeks, eyes were enucleated and optic nerves collected, post-fixed, processed and analysed by transmission electron microscopy. At low magnification electron-dense structures (arrow heads, a and b) were less frequent in the AAV-*ND11* + rotenone (a) treated samples compared with the AAV-*EGFP* + rotenone-treated samples (b). AAV-*EGFP* + rotenone-treated samples at higher magnification (c). (d) Bar chart representing mean number of membrane debris. Black and white columns represent AAV-*ND11* + rotenone (*ND11*) and AAV-*EGFP* + rotenone (*EGFP*), respectively. (e) Bar chart representing mean optic nerve diameter measurements. Optic nerves from identically injected mice were taken 9 months post-rotenone treatment, fixed, cryosectioned ($12 \mu\text{m}$), and the thickness of the optic nerve measured using light microscopy. Black and white columns represent AAV-*ND11* + rotenone (*ND11*) and AAV-*EGFP* + rotenone (*EGFP*), respectively. Error bars represent SD values and $**P < 0.01$. Scale bars: $10 \mu\text{m}$ (a–c) and $2 \mu\text{m}$ (d).

voltage-gated calcium channels²⁸ and hence provides insights into the integrity of calcium channels. Adult mice were intravitreally injected in one eye with 3×10^9 vp AAV-*ND11* ($n=10$). Three weeks post-injection, 1.5 nmol of rotenone was administered intravitreally to the same eye. A further group of adult animals received either an intravitreal injection of 1.5 nmol of rotenone ($n=10$) or vehicle alone (DMSO, $n=10$) in one eye. One week post-rotenone

(or DMSO) administration mice were given $40 \mu\text{g}$ of MnCl_2 intravitreally (20mg/ml in PBS) into the treated eye and optic nerve function was analysed by measuring MEMRI signal 2 h later (Figure 4). MEMRI signals in mice that had received rotenone (Figure 4c) showed significantly decreased contrasting in the optic nerve region immediately superior to the optic chiasmata (green) in comparison with control mice administered with DMSO alone

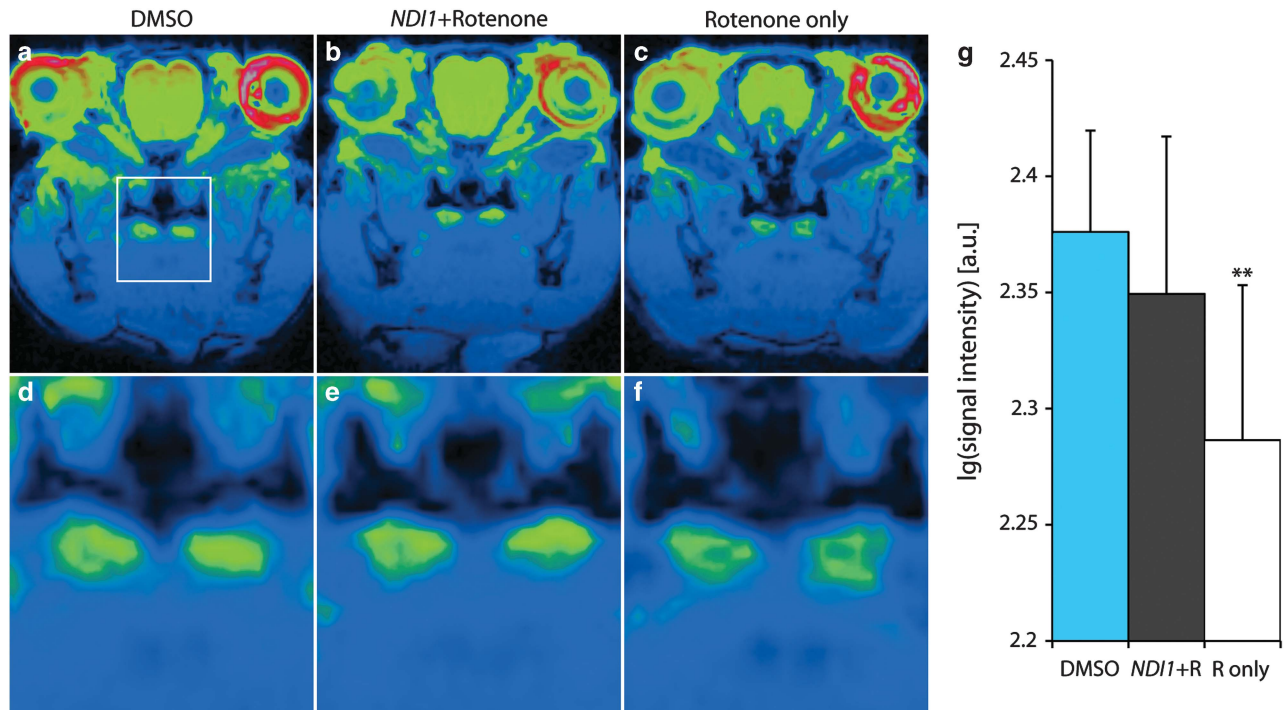


Figure 4 Functional analysis of *ND11*-treated optic nerves following rotenone insult. Right eyes of adult wild-type mice were intravitreally injected with AAV-*ND11* ($n=10$). After 3 weeks, AAV-*ND11* ($n=10$) injected mice received 1.5 nmol rotenone in the right eye. A further group of adult wild-type mice received either DMSO (vehicle control, $n=10$) or 1.5 nmol rotenone intravitreally injected into the right eye ($n=10$). Two weeks post-rotenone, or DMSO, treatment each mouse was intravitreally injected with 40 μg MnCl_2 and MEMRI carried out 2 h later. Pseudo-coloured T_1 -weighted images: signal enhancement of the mouse visual pathway in oblique sections (36°) from DMSO (a), AAV-*ND11* + rotenone (b) and rotenone alone (c) are presented. (d–f) Correspond to the marked area in a (the area of the optic chiasm) and corresponding areas in b and c, respectively. (g) Bar chart representing mean lg signal intensities in the region of the optic chiasm calculated using the Image J software. a.u., arbitrary unit. Error bars represent SD values and ** represent $P < 0.01$.

(Figure 4a, 2.2864 ± 0.067 and 2.376 ± 0.044 units, respectively, $P < 0.001$, $n = 10$). The reduction in MEMRI signal intensity suggests that the rotenone-induced damage to the RGCs observed previously using histological assays (Figure 2) may have blocked the active transport of Mn^{2+} using calcium channels in the optic nerve cells. In contrast to rotenone mice, mice injected with both AAV-*ND11* and rotenone displayed significantly more contrasting of the optic chiasm (Figure 4b, 2.3494 ± 0.068 units, $P < 0.01$, $n = 10$). This was comparable to levels seen in control mice that had received DMSO alone (2.376 ± 0.044 units, $n = 10$), suggesting that intravitreal administration of AAV-*ND11* was beneficial for optic nerve function.

In addition, we explored whether the histological and functional benefits obtained with AAV-*ND11* in this model of LHON in the retina and optic nerve translated to improved spatial vision. Contralateral eyes of adult mice were intravitreally injected with 3×10^9 vp AAV-*ND11* or 3×10^9 vp AAV-*EGFP* ($n = 8$). Three weeks post-injection, 1.5 nmol of rotenone was administered intravitreally to both eyes. OKR were measured³³ and the spatial frequency threshold, the point at which an animal no longer tracks the moving grating, was established separately for eyes treated with either AAV-*ND11* or control eyes treated with AAV-*EGFP*, 3 months post-rotenone treatment (Figure 5). AAV-*ND11*-treated eyes displayed significantly better optokinetic tracking responses than those treated with AAV-*EGFP* (0.384 ± 0.021 and 0.271 ± 0.034 cyc/deg, respectively, $P < 0.001$, $n = 8$). Indeed the spatial frequency of eyes treated with AAV-*ND11* and rotenone mirrored that of eyes treated with virus alone (AAV-*ND11*; 0.3870 ± 0.017 or AAV-*EGFP*; 0.403 ± 0.016). These data demonstrate that intravitreal administration of

AAV-*ND11* not only provided morphological and functional benefit, but also preserved mouse vision in the presence of the complex I inhibitor rotenone.

DISCUSSION

LHON is a debilitating and currently untreatable retinal degeneration. The development of gene therapies for LHON has been hampered by the mitochondrial mode of inheritance, intragenic heterogeneity, the need to deliver a therapy to the RGC layer and a scarcity of animal models for the disease.¹¹ With regard to the latter, novel mitochondrial gene replacement methodologies in stem cells may aid with the developing animal models for mitochondrial diseases in the future.³⁶ Rotenone has been used to generate chemically induced models for a number of disorders, including PD, AD and LHON.^{12–16} As demonstrated in this study, intravitreal injection of 1.5 nmol of rotenone into wild-type (129S2/SvHsd) mice induced RGC loss, optic nerve degeneration and significantly affected visual function, as assessed by MEMRI and OKR, simulating many features of human LHON (see controls in Figures 2–5).

ND11, a nuclear-encoded yeast equivalent to mammalian complex I, has been proposed as a potential therapeutic for diseases associated with complex I dysfunction, including PD and LHON.^{9,10} AAV-*ND11* appears to be well tolerated in rat brain and muscle as no detectable quantity of anti-Nd11 antibody was present in sera 6 months post-injection.³⁷ Although previous studies demonstrate the potential of *ND11*-based therapies for LHON, injection of the viral therapy directly into the brain is unlikely to be readily translatable to human LHON patients. In contrast, intravitreal AAV-*ND11* delivery,

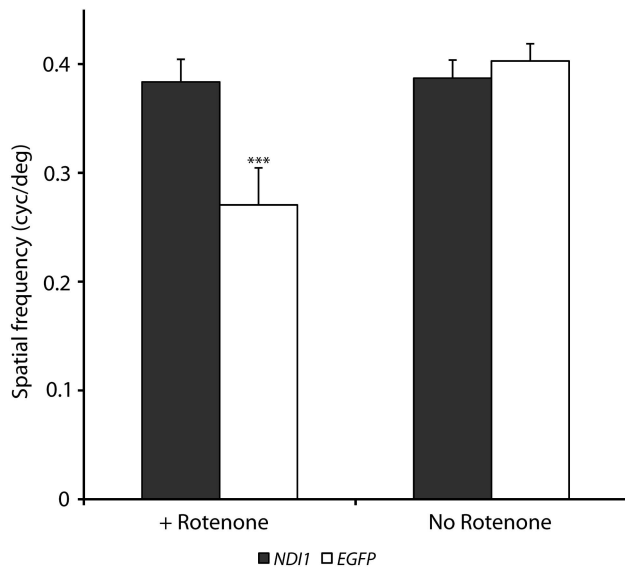


Figure 5 Analysis of spatial vision in *NDI1*-treated mice following rotenone insult. Adult wild-type mice were intravitreally injected into contralateral eyes with 3×10^9 vp AAV-*NDI1* or 3×10^9 vp AAV-*EGFP*. Three weeks post-injection, 1.5 nmol of rotenone was administered intravitreally to both eyes; control mice were not administered with rotenone. Three months post-rotenone treatment OKR were measured using a VOS. Bar chart represents the mean spatial frequency threshold established for each eye. Black and white columns represent values corresponding to AAV-*NDI1* + rotenone (*NDI1*) and AAV-*EGFP* + rotenone (*EGFP*), respectively, in rotenone-treated (+ Rotenone) and control (no Rotenone) mice. Error bars represent SD values and *** $P < 0.001$.

as explored in this study, represents a directly translatable clinical approach.

We describe a mutation-independent therapy for LHON utilising *NDI1*, which overcomes intragenic heterogeneity and is delivered directly to the target RGCs by intravitreal injection. AAV2/2 was the vector of choice as this serotype transduces RGCs efficiently.^{18–20} Of note, AAV2/2 expressing the *RPE65* gene has been used in human clinical trials for LCA and has been shown to be well tolerated in the human eye^{38–42} for over 3 years post-treatment. In this study, intravitreal injection of AAV-*NDI1* provided substantial protection against rotenone-induced insult (Figures 2–5). Notably, histological analyses demonstrated significant protection of both RGCs and the optic nerve (Figures 2 and 3). Furthermore, MEMRI indicated that AAV-*NDI1* treatment preserved optic nerve function by enabling active transport of Mn^{2+} through the optic nerve using voltage-gated calcium channels and hence provided evidence of improved functional integrity of the optic nerve tissue in AAV-*NDI1*-treated eyes compared with control eyes (Figure 4). Evaluation of visual function by optokinetics showed that the protection of RGCs and optic nerve integrity afforded by AAV-*NDI1* led to preservation of mouse vision in the presence of the rotenone (Figure 5). The results highlight the potential therapeutic value of *NDI1*-based therapies for LHON when intravitreally delivered using AAV2/2.

Alternative therapeutic approaches are being considered for LHON. For example, preclinical studies in which benefit was demonstrated have been undertaken for a *ND4*-related LHON gene therapy.⁴³ Introduction of the human *ND4* gene harbouring the G11778A mutation by electroporation⁴³ or AAV⁴⁴ to the murine vitreal cavity resulted in a phenotype similar to LHON. Subsequent electroporation with a wild-type *ND4* gene prevented RGC loss and visual

impairment.⁴³ It will be of value to establish if addition of wild-type *ND4* to human *ND4*-linked LHON patients many of whom do not express any wild-type *ND4* in RGCs, unlike the murine models, will be therapeutically beneficial.⁴⁵ Screening of LHON patients for *ND4* mutations is being undertaken in the University of Miami in preparation for clinical trials, planned to commence within the next 4 years.⁴⁶

As for many neurodegenerative disorders a variety of neurotrophic factors and anti-oxidants are being explored as therapies.^{47–51} Santhera's quinone-based drug termed idebenone (a coenzyme Q10 analogue), initially targeted towards AD and Duchenne Muscular Dystrophy is currently in a Phase III trial for LHON.⁴⁸ Although the beneficial effects thus far may be somewhat modest, to patients suffering the devastating vision loss characteristic of LHON, they are welcome. In addition, an array of neuroprotective agents and anti-oxidants such as memantine and valproic acid^{49–51} are being considered as treatments for LHON and other optic nerve degenerations.

In this study, AAV-*NDI1* was used to treat a murine model of LHON and significant benefit demonstrated using both histological and functional assays. A clear advantage of using the *NDI1* gene over allotopic expression of mammalian mitochondrial complex I subunit genes as a therapy for LHON is that a single gene may provide benefit to all LHON patients with a complex I deficiency irrespective of which complex I subunit gene is causative of this debilitating retinopathy. In addition, unlike these complex I subunit genes, *NDI1* is expressed in the nucleus of yeast and contains an endogenous MLS to facilitate import of protein into mitochondria. Hence, transport of *Ndi1* protein to mitochondria is naturally optimised and may be more efficient than transport of allotopically expressed therapeutic genes with introduced MLSs. Of note, intravitreal administration of AAV-*NDI1*, which efficiently transduces RGCs, may be directly applicable to human patients with LHON, given that AAV2 is well tolerated in the human eye^{38–42} and intravitreal injection in humans is a routine procedure.⁵² A tissue-specific promoter may be used in future studies to further enhance the therapy. In summary, the data obtained from the study represent a significant step in progressing AAV2-*NDI1*-based therapeutics towards the clinic for this debilitating mitochondrially inherited eye disorder, which typically affects young males in their most productive years.

CONFLICT OF INTEREST

GJF and PK are directors of Genable Technologies; SM-W, NC, AP and MO'R are consultants for Genable Technologies. The remaining authors declare no conflict of interest.

ACKNOWLEDGEMENTS

We thank Dr Christian Kerskens (Trinity College Dublin) for his advice with MRI experiments, Prof Richard Porter and Lars Manzke (Trinity College Dublin) for their advice on respiratory analysis experiments, Gavin MacManus (Trinity College Dublin) for assistance with confocal microscopy, the staff of the Bioresources Unit (Trinity College Dublin) and Elisabeth Sehn (Johannes Gutenberg University) for skilful technical assistance. The research was supported by grant awards from Fighting Blindness Ireland, Science Foundation Ireland, Irish Research Council for Science, Engineering & Technology, Deutsche Forschungsgemeinschaft (GRK1044), FAUN-Stiftung and BMBF 'Hope'.

1 Yu-Wai-Man P, Griffiths PG, Chinnery PF: Mitochondrial optic neuropathies – disease mechanisms and therapeutic strategies. *Prog Retin Eye Res* 2011; **30**: 81–114.

- 2 Chalmers RM, Schapira AH: Clinical biochemical and molecular genetic features of Leber's hereditary optic neuropathy. *Biochim Biophys Acta* 1999; **1410**: 147–158.
- 3 Mackey DA, Oostra RJ, Rosenberg T *et al*: Primary pathogenic mtDNA mutations in multigeneration pedigrees with Leber hereditary optic neuropathy. *Am J Hum Genet* 1996; **59**: 481–485.
- 4 Jarrett SG, Lin H, Godley BF, Boulton ME: Mitochondrial DNA damage and its potential role in retinal degeneration. *Prog Retin Eye Res* 2008; **27**: 596–607.
- 5 Ames III A: CNS energy metabolism as related to function. *Brain Res Brain Res Rev* 2000; **34**: 42–68.
- 6 Yen MY, Wang AG, Wei YH: Leber's hereditary optic neuropathy: a multifactorial disease. *Prog Retin Eye Res* 2006; **25**: 381–396.
- 7 Porter RK, Joyce OJ, Farmer MK *et al*: Indirect measurement of mitochondrial proton leak and its application. *Int J Obes Relat Metab Disord* 1999; **23**(Suppl 6): S12–S18.
- 8 Kitajima-Ihara T, Yagi T: Rotenone-insensitive internal NADH-quinone oxidoreductase of *Saccharomyces cerevisiae* mitochondria: the enzyme expressed in *Escherichia coli* acts as a member of the respiratory chain in the host cells. *FEBS Lett* 1998; **421**: 37–40.
- 9 Marella M, Seo BB, Yagi T, Matsuno-Yagi A: Parkinson's disease and mitochondrial complex I: a perspective on the Ndi1 therapy. *J Bioenerg Biomembr* 2009; **41**: 493–497.
- 10 Marella M, Seo BB, Thomas BB, Matsuno-Yagi A, Yagi T: Successful amelioration of mitochondrial optic neuropathy using the yeast NDI1 gene in a rat animal model. *PLoS One* 2010; **5**: e11472.
- 11 Manfredi G, Beal MF: Poison and antidote: a novel model to study pathogenesis and therapy of LHON. *Ann Neurol* 2004; **56**: 171–172.
- 12 Betarbet R, Sherer TB, MacKenzie G, Garcia-Osuna M, Panov AV, Greenamyre JT: Chronic systemic pesticide exposure reproduces features of Parkinson's disease. *Nat Neurosci* 2000; **3**: 1301–1306.
- 13 Mulcahy P, Walsh S, Paucard A, Rea K, Dowd E: Characterisation of a novel model of Parkinson's disease by intra-striatal infusion of the pesticide rotenone. *Neuroscience* 2011; **181**: 234–242.
- 14 Ullrich C, Humpel C: Rotenone induces cell death of cholinergic neurons in an organotypic co-culture brain slice model. *Neurochem Res* 2009; **34**: 2147–2153.
- 15 Zhang X, Jones D, Gonzalez-Lima F: Mouse model of optic neuropathy caused by mitochondrial complex I dysfunction. *Neurosci Lett* 2002; **326**: 97–100.
- 16 Zhang X, Jones D, Gonzalez-Lima F: Neurodegeneration produced by rotenone in the mouse retina: a potential model to investigate environmental pesticide contributions to neurodegenerative diseases. *J Toxicol Environ Health A* 2006; **69**: 1681–1697.
- 17 Hayworth CR, Rojas JC, Gonzalez-Lima F: Transgenic mice expressing cyan fluorescent protein as a reporter stain to detect the effects of rotenone toxicity on retinal ganglion cells. *J Toxicol Environ Health A* 2008; **71**: 1582–1592.
- 18 Dudas L, Anand V, Acland GM *et al*: Persistent transgene product in retina, optic nerve and brain after intraocular injection of rAAV. *Vision Res* 1999; **39**: 2545–2553.
- 19 Harvey AR, Kamphuis W, Eggers R *et al*: Intravitreal injection of adeno-associated viral vectors results in the transduction of different types of retinal neurons in neonatal and adult rats: a comparison with lentiviral vectors. *Mol Cell Neurosci* 2002; **21**: 141–157.
- 20 Lukason M, DuFresne E, Rubin H *et al*: Inhibition of choroidal neovascularisation in a nonhuman primate model by intravitreal administration of an AAV2 vector expressing a novel anti-VEGF molecule. *Mol Ther* 2011; **19**: 260–265.
- 21 Klimczak RR, Koerber JT, Dalkara D, Flannery JG, Schaffer DV: A novel adeno-associated viral variant for efficient and selective intravitreal transduction of rat Müller cells. *PLoS One* 2009; **4**: e7467.
- 22 Yamashita T, Nakamaru-Ogiso E, Miyoshi H, Matsuno-Yagi A, Yagi T: Roles of bound quinone in the single subunit NADH-quinone oxidoreductase (Ndi1) from *Saccharomyces cerevisiae*. *J Biol Chem* 2007; **282**: 6012–6020.
- 23 Levitt N, Briggs D, Gil A, Proudfoot NJ: Definition of an efficient synthetic poly(A) site. *Genes Dev* 1989; **3**: 1019–1025.
- 24 Palfi A, Millington-Ward S, Chadderton N *et al*: Adeno-associated virus-mediated rhodopsin replacement provides therapeutic benefit in mice with a targeted disruption of the rhodopsin gene. *Hum Gene Ther* 2010; **21**: 311–323.
- 25 O'Reilly M, Palfi A, Chadderton N *et al*: RNA interference-mediated suppression and replacement of human rhodopsin *in vivo*. *Am J Hum Genet* 2007; **81**: 127–135.
- 26 Chadderton N, Millington-Ward S, Palfi A *et al*: Improved retinal function in a mouse model of dominant retinitis pigmentosa following AAV-delivered gene therapy. *Mol Ther* 2009; **17**: 593–599.
- 27 Wolfrum U: Cytoskeletal elements in arthropod sensilla and mammalian photoreceptors. *Biol Cell* 1992; **176**: 373–381.
- 28 Lin YJ, Koretsky AP: Manganese ion enhances T1-weighted MRI during brain activation: an approach to direct imaging of brain function. *Magn Reson Med* 1997; **38**: 378–388.
- 29 Watanabe T, Michaelis T, Frahm J: Mapping of retinal projections in the living rat using high-resolution 3D gradient-echo MRI with Mn2+ -induced contrast. *Magn Reson Med* 2001; **46**: 424–429.
- 30 Lindsey JD, Scadeng M, Dubowitz DJ, Crowston JG, Weinreb RN: Magnetic resonance imaging of the visual system *in vivo*: transsynaptic illumination of V1 and V2 visual cortex. *Neuroimage* 2007; **34**: 1619–1626.
- 31 Bearer EL, Falzone TL, Zhang X, Biris O, Rasin A, Jacobs RE: Role of neuronal activity and kinesin on tract tracing by manganese-enhanced MRI (MEMRI). *Neuroimage* 2007; **37**(S1): S37–S46.
- 32 Abramoff MD, Magalhaes PJ, Ram SJ: Image processing with ImageJ. *Biophotonics International* 2004; **11**: 36–42.
- 33 Prusky GT, Alam NM, Beekman S, Douglas RM: Rapid quantification of adult and developing mouse spatial vision using a virtual optomotor system. *Invest Ophthalmol Vis Sci* 2004; **45**: 4611–4616.
- 34 Williams RW, Strom RC, Rice DS, Goldowitz D: Genetic and environmental control of variation in retinal ganglion cell number in mice. *J Neurosci* 1996; **16**: 7193–7205.
- 35 Seo BB, Kitajima-Ihara T, Chan EK, Scheffler IE, Matsuno-Yagi A, Yagi T: Molecular remedy of complex I defects: rotenone-insensitive internal NADH-quinone oxidoreductase of *Saccharomyces cerevisiae* mitochondria restores the NADH oxidase activity of complex I-deficient mammalian cells. *Proc Natl Acad Sci USA* 1998; **95**: 9167–9171.
- 36 Iyer S, Xiao E, Alsayegh K, Eroshenko N, Riggs MJ, Bennett Jr JP, Rao RR: Mitochondrial gene replacement in human pluripotent stem cell-derived neural progenitors. *Gene Ther* 2012; **19**: 469–475.
- 37 Marella M, Seo BB, Flotte TR, Matsuno-Yagi A, Yagi T: No immune responses by the expression of the yeast ndi1 protein in rats. *PLoS One* 2011; **6**: e25910.
- 38 Bainbridge JW, Smith AJ, Barker SS *et al*: Effect of gene therapy on visual function in Leber's congenital amaurosis. *N Engl J Med* 2008; **358**: 2231–2239.
- 39 Maguire AM, Simonelli F, Pierce EA *et al*: Safety and efficacy of gene transfer for Leber's congenital amaurosis. *N Engl J Med* 2008; **358**: 2240–2248.
- 40 Cideciyan AV, Aleman TS, Boye SL *et al*: Human gene therapy for RPE65 isomerase deficiency activates the retinoid cycle of vision but with slow rod kinetics. *Proc Natl Acad Sci USA* 2008; **105**: 15112–15117.
- 41 Simonelli F, Maguire AM, Testa F *et al*: Gene therapy for Leber's congenital amaurosis is safe and effective through 1.5 years after vector administration. *Mol Ther* 2010; **18**: 643–650.
- 42 Jacobson SG, Cideciyan AV, Ratnakaram R *et al*: Gene therapy for leber congenital amaurosis caused by RPE65 mutations: safety and efficacy in 15 children and adults followed up to 3 years. *Arch Ophthalmol* 2012; **130**: 9–24.
- 43 Ellouze S, Augustin S, Bouaita A *et al*: Optimized allotropic expression of the human mitochondrial ND4 prevents blindness in a rat model of mitochondrial dysfunction. *Am J Hum Genet* 2008; **83**: 373–387.
- 44 Qi X, Sun L, Lewin AS, Hauswirth WW, Guy J: The mutant human ND4 subunit of complex I induces optic neuropathy in the mouse. *Invest Ophthalmol Vis Sci* 2007; **48**: 1–10.
- 45 Smith AJ, Bainbridge JW, Ali RR: Gene supplementation therapy for recessive forms of inherited retinal dystrophies. *Gene Ther* 2012; **19**: 154–161.
- 46 Lam BL, Feuer WJ, Abukhalil F, Porciatti V, Hauswirth WW, Guy J: Leber hereditary optic neuropathy clinical trial recruitment: year 1. *Arch Ophthalmol* 2010; **128**: 1129–1135.
- 47 Qi X, Lewin AS, Sun L, Hauswirth WW, Guy J: SOD2 gene transfer protects against optic neuropathy induced by deficiency of complex I. *Ann Neurol* 2004; **56**: 182–191.
- 48 Klopstock T, Yu-Wai-Man P, Dimitriadis K *et al*: A randomized placebo-controlled trial of idebenone in Leber's hereditary optic neuropathy. *Brain* 2011; **134**(Part 9): 2677–2686.
- 49 Rojas JC, Lee J, John JM, Gonzalez-Lima F: Neuroprotective effects of near-infrared light in an *in vivo* model of mitochondrial optic neuropathy. *J Neurosci* 2008; **28**: 13511–13521.
- 50 Biermann J, Grieshaber P, Goebel U, Martin G, Thanos S, Di Giovanni S: Valproic acid-mediated neuroprotection and regeneration in injured retinal ganglion cells. *Invest Ophthalmol Vis Sci* 2010; **51**: 526–534.
- 51 Biermann J, Boyle J, Pielen A, Lagrèze WA: Histone deacetylase inhibitors sodium butyrate and valproic acid delay spontaneous cell death in purified rat retinal ganglion cells. *Mol Vis* 2011; **17**: 395–403.
- 52 Doshi RD, Bakri SJ, Fung AE: Intravitreal Injection Technique. *Sem Ophthalmol* 2011; **26**: 104–113.



This work is licensed under the Creative Commons Attribution-NonCommercial-No Derivative Works 3.0 Unported License. To view a copy of this license, visit <http://creativecommons.org/licenses/by-nc-nd/3.0/>

Supplementary Information accompanies the paper on European Journal of Human Genetics website (<http://www.nature.com/ejhg>)